Transient Outward K^+ Channels in Vesicles Derived from Frog Skeletal Muscle Plasma Membranes

J. Camacho,* M. J. Delay,# M. Vazquez,§ C. Argüello,‖ and J. A. Sánchez*
Departments of *Pharmacology and Toxicology and ‖Pathology, Centro de Investigación y de Estudios Avanzados del IPN, Mexico D.F., Mexico; §Department of Physiology, School of Medicine, UNAM, Mexico D.F., Mexico; and #Axon Instruments, Foster City, California 94404 USA

ABSTRACT Whole-cell voltage-clamp experiments were performed in vesicles derived from frog skeletal muscle plasma membranes. Capacitance measurements showed that these vesicles lack invaginations. In solutions containing K^+, transient outward currents with reversal potentials close to E_K were recorded with a maximum potassium conductance of 0.3 mS/cm^2. These currents inactivated in a voltage-dependent manner with a time constant of decay that reached a limiting value of 26 ms at large depolarizations. The steady-state inactivation reached half-maximum values at −66 mV. Transient currents were completely blocked with 5 mM 4-aminopyridine. Single-channel recordings made in inside-out excised patches from the vesicles had ensemble averages with characteristics similar to those of the macroscopic currents, although with significantly faster inactivation time constants. The single-channel chord conductance was 21 pS when the pipette and bath solutions contained 2.5 mM and 120 mM KCl, respectively. It is concluded that these vesicles contain potassium channels that are very similar to A channels found in neurons and other cells.

INTRODUCTION

Many types of potassium channels are found in excitable cells. Despite this diversity, potassium channels carrying transient outward currents are ubiquitous and are present in many cells, such as neurons, sensory cells, heart cells, *Drosophila* flight muscles, and primitive metazoan organisms (see Rogawski, 1985; Rudy, 1988). Originally described in neurons (Hagiwara et al., 1961), currents flowing through these channels are commonly referred to as A currents (Connor and Stevens, 1971).

Although the presence of this type of potassium channel is a characteristic feature of many excitable cells, there are no reports describing A currents in vertebrate skeletal muscle fibers. Other types of potassium channels, such as delayed rectifier channels similar to those found in axons and neurons, Ca-activated and inward rectifier potassium channels, have been described in skeletal muscle (Hodgkin and Horowicz, 1959; Adrian et al., 1970; Blatz and Magleby, 1984).

This paper describes whole-cell and single-channel voltage-clamp experiments in vesicles obtained by enzymatic treatment of frog skeletal muscle cells. We found that transient potassium currents are present in the vesicles and that they are similar to A currents recorded in other preparations.

As A currents have not been reported previously in skeletal muscle, we calculated the hypothetical time course and amplitude of A currents in the intact preparation, based on measurements made in vesicles. Indirect evidence (see Materials and Methods) suggests that the vesicle membranes may derive from membranes of the transverse tubular (T) system. Under this assumption, vesicular A currents were extrapolated to a muscle fiber using a simulation of the cable properties of the T-system. The hypothetical currents so estimated are sufficiently large that they could not have been overlooked in intact muscle fibers, suggesting that they may be suppressed under normal conditions.

Preliminary results have been published (Camacho and Sánchez, 1993).

MATERIALS AND METHODS

Preparation

Spherical vesicles were derived from the plasma membrane of skeletal muscle of the frog *Rana montezumae*. Frogs were killed by decapitation. The procedure of vesicle formation by enzymatic treatment was similar to the one described by Standen et al. (1984). Semitendinosus or sartorius muscles were incubated in 120 mM KCl (solution C, Table 1) with added collagenase (Type IA, 50 units/ml; Sigma Chemical Co., St. Louis, MO) but without protease treatment. Vesicles formed spontaneously after a period of about 60 min.

Solutions

Table 1 shows the solutions employed for measurements of passive properties of the vesicles and of K^+ currents. Solutions B and E were used in all experiments to measure K^+ currents in whole-cell recordings. Tetrodotoxin (1 μM) was used to block Na^+ channels. Extracellular and intracellular solutions were buffered with HEPES (5 mM) at pH 7.2 and 7.1, respectively. All chemicals were obtained from either Sigma Chemical Co. or Aldrich Chemical Co. (St. Louis, MO). Experiments were carried out at room temperature, 20–22°C.

Electrophysiological methods

The patch-clamp technique was used in the whole-cell and in the inside-out configurations (Hamill et al., 1981). Pipettes were double-pulled from hard

Received for publication 9 November 1995 and in final form 15 April 1996.
Address reprint requests to Dr. Jorge A. Sánchez, Department of Pharmacology and Toxicology, CINVESTAV, Mexico, D.F., Apartado Postal 14-740, Mexico, 07000. Tel.: 525-747-7000, ext. 5413; Fax: 525-577-7090; E-mail: jsanchez@mvax1.red.cinvestav.mx.

0006-3495/96/07/171/11 $2.00

TABLE 1 Composition of solutions (mM)

	Bath solutions, pH = 7.2 (HEPES)							
	K^+	TEA^+	TMA^+	Ca^{2+}	Mg^{2+}	Cl^-	$CH_3SO^-_3$	EGTA
A	—	110	—	10	—	20	110	—
B	27	—	106	—	5	143	—	—
C	120	—	—	—	2	124	—	1
	Pipette solutions, pH = 7.1 (HEPES)							
	K^+	Cs^+	Na^+	Mg^{2+}	Ca^{2+}	Cl^-	$CH_3SO^-_3$	EGTA
D	—	120	—	2	—	4	120	1
E	120	—	—	2	—	124	—	1
F	2.5	—	117.5	—	2	124	—	—

glass (KIMAX-51; Kimble Glass, Toledo, OH) using a David Kopf vertical puller (model 700; Tujunga, CA). This particular type of glass was selected because it does not cause artifactual inactivation as has been observed with soft glass that may release water-soluble components (Cota and Armstrong, 1988). The tips of electrodes for use in single-channel experiments were coated with Sylgard (Dow Corning, Midland, MI). All electrodes were fire-polished to resistances of about 6–8 MΩ. The mean series resistance with these patch-clamp pipettes in whole-cell experiments was 10.5 ± 2.3 MΩ (n = 7). Series resistance compensation was used to cancel 70–90% of the series resistance. Maximum membrane currents reached values of up to 3 nA, yielding values within 3 mV for the voltage drop across the series resistance. For a vesicle capacitance of 80 pF (see Results), the calculated settling time for the clamp is 800 μs.

Whole-cell recordings in vesicles were achieved by rupturing the patch of membrane in the pipette by suction in a manner similar to that used in cells. However, although gigaseal formation was achieved routinely, great care was essential when further suction was applied. The vesicles were very fragile and their complete disruption occurred frequently, possibly because they lack cytoskeletal components (see below). This fragility also prevented the successful exchange of bath solutions. Although we attempted to use small vesicles, it was only possible to obtain stable recordings with large vesicles of about 50 μm diameter.

Data collection and pulse protocol

Membrane currents (I_m) in response to voltage step depolarizations applied from the holding potential (E_h) were measured with an EPC-7 amplifier (Adams and List, Westbury, NY) and sampled by an IBM-PC/AT-compatible 80386-based microcomputer. Analog signals were digitized to a resolution of 12 bits through a data acquisition interface (TL-1 Lab Master with DMA; Axon Instruments, Foster City, CA) that also generated the command pulses. Data were analyzed by pCLAMP (Version 5.5; Axon Instruments). I_m was amplified and filtered by an active four-pole low-pass Bessel filter with a corner frequency of no more than half the sampling frequency. To measure activation of K^+ currents (I_K), command pulses of 100–200 ms duration and variable amplitude were delivered. Linear components were subtracted by either of two procedures. In one method, linear currents were subtracted after appropriate scaling of membrane currents generated by a −20-mV pulse from the holding potential (E_h) that ranged between −80 and −100 mV. This pulse was delivered 200 ms before the corresponding test pulse. The other method employed subtraction of test currents from the sum of the currents generated by four consecutive pulses, each having one-fourth the amplitude of the test pulse and the same polarity (P/4 procedure).

Steady-state inactivation was investigated by delivering 1022-ms-long prepulses to several potentials followed by 100-ms test pulses to +40 mV.

The fitting of formulae to experimental data employed a nonlinear least-squares algorithm. Parameter values given in the tables are expressed as mean ± standard error.

Video microscopy of vesicles

Skeletal muscle fibers incubated as described above were placed on a slide and covered with a calibrated coverslip (0.17 mm). Muscle fibers and the production of vesicles were observed with a differential interference contrast microscope containing a 40× planachromatic objective. Images were recorded with a video CCD camera.

Transmission electron microscopy of vesicles

Samples of skeletal muscle fibers under enzymatic treatment were fixed for 1 h with 2.5% glutaraldehyde in 0.1 M sodium cacodylate buffer at pH 7.2 and postfixed with 1% osmium tetroxide in the same buffer. Fibers were dehydrated with increasing concentrations of ethanol, followed by two changes of propylene oxide and embedded in Epcon 812. Ultrathin sections stained with uranyl acetate and lead citrate were observed with a transmission electron microscope (EM-10; Carl Zeiss, Thornwood, NY).

Simulation of A currents in skeletal muscle T-system

As A currents have not been reported in skeletal muscle, it was of interest to estimate the hypothetical magnitude and time course of A currents in an intact single fiber, by extrapolating from the currents measured in the vesicles. Two pieces of evidence suggest that the vesicle membranes may derive from membranes of the T-system. First, Escobar and Vergara (1993) found that isolated toad skeletal muscle fibers, stained with rhod-2 conjugated with phosphatidylethanolamine, showed rhod-2 fluorescence only in bands corresponding to the T-system, and that formation of vesicles from these fibers was associated with an increase in fluorescence of the vesicles and concomitant extinction of T-system fluorescence. Second, ATP-sensitive K^+ channels, which are found in planar lipid bilayers to which transverse tubular membrane components have been added (Parent and Coronado, 1989), may effectively be markers for tubular membranes, and similar channels are present in the vesicles (Spruce et al., 1987).

The time course of the A current reported in this paper is dependent on applied voltage, as was evidenced by the responses to a series of steps to different activating voltages (see Results). Because T-system membrane potentials are not well controlled by rapid step changes in potential at the surface membrane (Vergara and Bezanilla, 1981; Heiny and Vergara, 1982), the extrapolation of A current time courses to the T-system cannot be performed in a straightforward manner. A simulation was therefore made of the hypothetical time course and amplitude of A currents in an intact fiber, in which a voltage-clamp pulse applied at the surface membrane was propagated down the radial cable equivalent to the T-system, and the A current at each radial location was calculated based on the amplitude and time course of the membrane voltage at that point, and on the measured A currents as described in the Results.

Simulation of the time course and amplitude of the tubular potential followed the method of Ashcroft et al. (1985), briefly summarized here. The equivalent circuit of the transverse tubule was a radially distributed cable consisting of a series of concentric circuit elements, each with a parallel resistance and a capacitance. The potential across the tubular membrane, $u(r, t)$, was solved for the following equation:

$$\frac{\bar{G}_L}{r}\frac{\delta}{\delta r}\left(r\frac{\delta u}{\delta r}\right) = \bar{G}_W u + \bar{C}_W\frac{\delta u}{\delta t}, \quad (1)$$

where $\bar{C}_W$, $\bar{G}_W$, and $\bar{G}_L$ are the T-system capacitance, wall conductance, and lumen conductivity per fiber volume. These are derived from C_W and G_W (respectively, T-system capacitance and wall conductance per T-system membrane area) and from G_L, the lumen conductivity, by the relations $\bar{C}_W = C_W\rho/\xi$, $\bar{G}_W = G_W\rho/\xi$, and $\bar{G}_L = G_L\rho\sigma$, where ρ is the ratio of T-system volume to fiber volume, ξ is the ratio of volume to surface area of the T-system, and σ is a network factor (see Ashcroft et al., 1985). The transformation of Eq. 1 into a finite-difference equation and its numerical integration using the Crank-Nicholson method was implemented in a computer program for IBM-PC developed and generously provided by J. A. Heiny.

The data records $i(V, t)$ for the currents shown in Fig. 2 were parametrized as a function of applied potential V and time t as follows. The rising phase of the records until the time to peak was modeled using

$$g(t) = g_{max}(V)\sin((\pi/2)(t/t_{max}(V)), \quad t < t_{max}, \quad (2)$$

where $g(t)$ is the conductance, related to vesicle current $i_{ves}(t)$ through $g = i_{ves}/(V - E_K)$; E_K is the reversal potential for the current. $g_{max}(V)$, the maximum conductance for the potential V, is g_K from Eq. 7 and was calculated using the parameter values shown in Table 3. $t_{max}(V)$ is the time to peak conductance, also dependent on V, according to

$$t_{max}(V) = A_1\exp(-(V - A_2)/A_3) + A_4. \quad (3)$$

The falling phase of the records for $i(t)$ was parameterized using

$$g(t) = g_{max}(V)\exp(-(t - t_{max})/\tau_{fall}(V)), \quad t > t_{max}, \quad (4)$$

with the falling phase time constant parametrized as

$$t_{fall}(V) = A_5\exp(-(V - A_6)/A_7) + A_8. \quad (5)$$

Values for A_i were obtained by least-squares fit to the data in Fig. 2 and are as follows: A_1 = 34.3 ms, A_2 = −40.0 mV, A_3 = 17.7 mV, A_4 = 8.7 ms, A_5 = 243 ms, A_6 = −50.0 mV, A_7 = 7.1 mV, and A_8 = 26.9 ms.

This parameterization allowed the calculation of the vesicle current i_{ves} as a function of potential and time. The vesicle current density over the vesicle membrane was then $J_{ves} = i_{ves}/4\pi R_{ves}^2$, where R_{ves} is the vesicle radius. If the intact skeletal muscle fiber is modeled as a cylinder of radius R_{fiber} and length L, the radial surface of which is voltage clamped, the surface area of the T-system membrane is $S_T = (\rho/\xi)\pi R_{fiber}^2 L$, and the expected A current in this volume would be $J_{ves}\,S_T$. However, because the voltage along the transverse tubule was not expected to be radially uniform, it was necessary to calculate the A current associated with the potential at each radius, for each instant of time, and integrate that current over the radius. The cylinder was therefore treated as a series of concentric tubes, of which one was at radius r with thickness dr and length L. The A current in this volume was approximated as $i_{ves}(r, t)(\rho/\xi)(L/2R_{ves}^2)r\,dr$, where $i_{ves}(r, t)$ is the radially dependent parameterized current for the potential present at radius r at time t. Treating these differential elements as discrete volumes with radius $r = jR_{fiber}/N$, where j is an integer between 1 and N, and summing over j, the resultant A current extrapolated to the skeletal muscle fiber cylinder is given by $i_A(t)$, where

$$i_A(t) = (\rho/\xi)(L/2)(R_{fiber}/(NR_{ves}))^2\sum_{j=1}^{N} j i_{ves}(r, t). \quad (6)$$

This calculation was performed for the vesicle data $i(V, t)$ shown in Fig. 2. The simulation employed the following values: C_W = 0.9 μF/cm², G_W = 0.04 mS/cm, G_L = 7 mS/cm², ρ = 0.0032, $\xi = 1.45 \times 10^{-6}$ cm, σ = 0.5 and 10 Ω-cm access resistance; these are identical or close to values used by Ashcroft et al. (1985). Values specific to this simulation were R_{fiber} = 50 μm, L = 100 μm, N = 15, a calculation time interval of 10 μs, and a temperature of 21°C. The applied surface potential was assumed to be stepwise, and no conductances other than the leak were assumed to be present in the T-system.

RESULTS

Passive membrane properties of vesicles

Before recording ionic currents from the vesicles, it was important to characterize some of their passive membrane properties. Fig. 1 *A* illustrates fast capacitative transients associated with stray capacitance of the pipette after the formation of a gigaseal. These transients were completely compensated as illustrated. In Fig. 1 *B*, membrane currents were recorded after the application of moderate suction to the pipette, causing rupture of the membrane. Occurrence of rupture was indicated by the appearance of large membrane capacity transients produced by the application of pulses to the potentials indicated. The membrane capacitance of the vesicles was calculated by integration of current transients over time in solutions containing mostly impermeant ions (solutions A and D in Table 1). Fig. 1 *C* shows the mobilized charge during the "on" (empty circles) and "off" (filled circles) transients as a function of membrane potential. Data points were fitted to a straight line, the slope of which gives the value of the vesicle capacitance. No difference was observed between the "on" or "off" charges, indicating the absence of ionic currents under these experimental conditions.

Table 2 summarizes the passive properties of the vesicles from experiments similar to that of Fig. 1. The expected membrane capacitance was calculated assuming that the vesicles were spherical and had a specific capacitance of 1 μF/cm². The ratio between the measured and expected membrane capacitances was very close to 1, indicating that vesicles lack invaginations.

Transient K^+ currents in vesicles

The presence of K^+ channels in the vesicles became evident when we performed whole-cell experiments in K^+-containing solutions (B and E in Table 1). Fig. 2 illustrates membrane currents to the potentials indicated. For small depolarizations ionic currents were essentially linear and were canceled using the P/4 procedure. With a larger depolarization (−40 mV), an inward current was apparent that became outward with further depolarizations. These nonlinear cur-

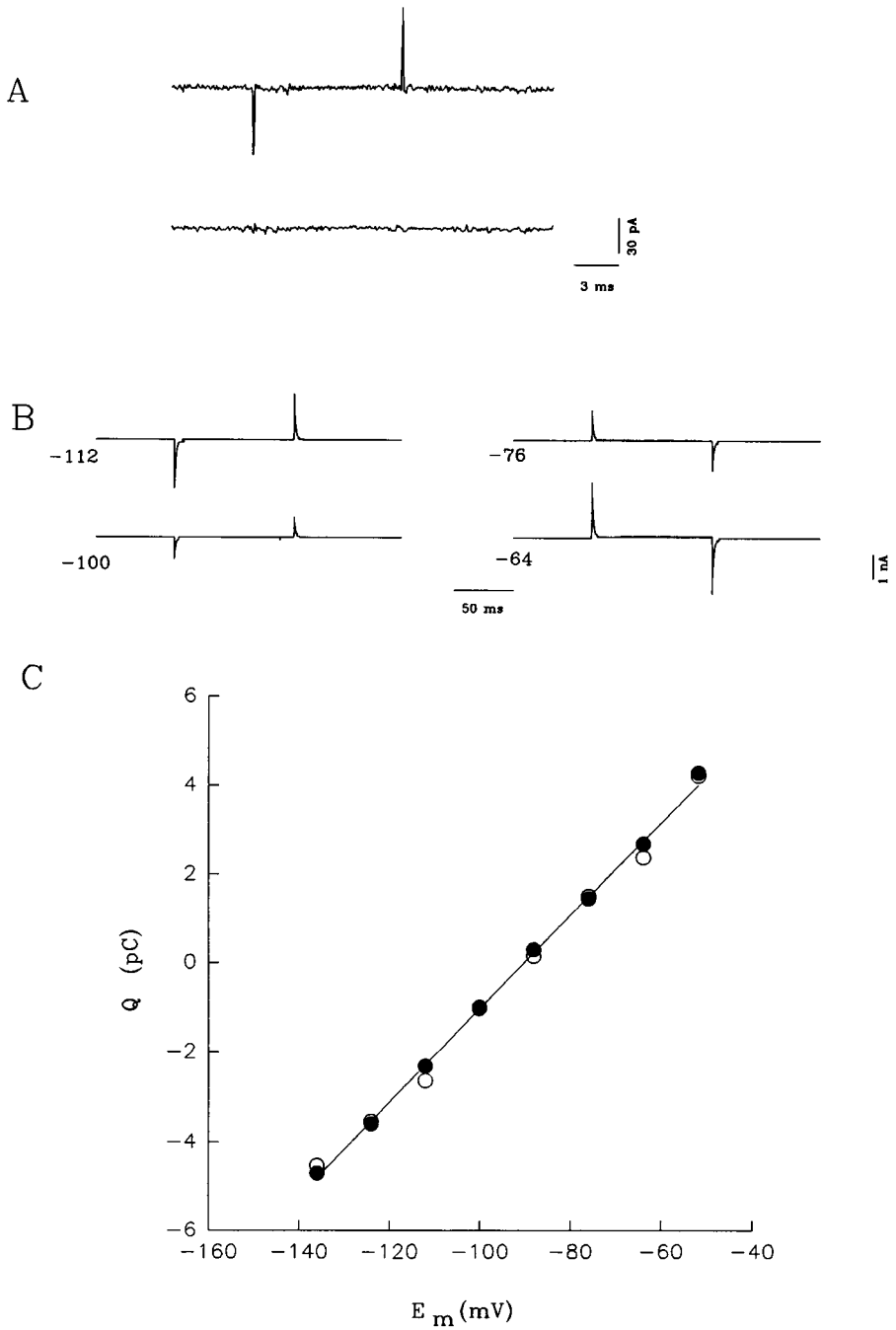

FIGURE 1 Whole cell, voltage-clamp recordings in vesicles. (*A*) Records made after the formation of a gigaseal before and after stray capacitance compensation. (*B*) "Whole cell" membrane currents in solutions containing impermeant ions (solutions A and D in Table 1). No membrane capacitance compensation was used. $E_h = -90$ mV. Note that the amplitude scale in *B* differs from that in *A*. (*C*) Charge-voltage relation. ○, Integration of "on" transients; ●, integration of "off" transients. The straight line is the least-squares fit to the data points, with a slope of 104.9 pF. The correlation coefficient of the fit was 0.999. Same experiment throughout.

rents did not persist but inactivated completely during the pulse. The reversal potential of −33 mV, calculated by linear interpolation, was close to E_K (−37.5 mV), indicating that currents are carried by this cation. Transient I_K were always present in vesicles recorded under similar experimental conditions, although sometimes currents did not decline to zero but instead showed a steady component.

Fig. 3 *A* shows the current-voltage relation from the experiment illustrated in Fig. 2. Activation of K^+ currents began at about −50 mV. Values of the corresponding potassium conductance ($g_K = I_K/(E_m - E_K)$) are plotted in Fig. 3 *B* as a function of membrane potential E_m. For descriptive purposes, the points in Fig. 3 *B* were fitted to a two-state Boltzmann distribution:

$$g_K = g_{K,max}/[1 + \exp((-E_m + \bar{V})/k)], \quad (7)$$

with the parameters indicated in the legend, where $g_{K,max}$ is the maximum conductance per unit area, $\bar{V}$ is the potential at which the conductance reaches its half-maximum value, and k is a measure of the steepness. The associated membrane conductance saturates at large depolarizations. To calculate the rate of inactivation of K^+ currents shown in Fig. 2, the decaying phase of I_K was fitted to a single

TABLE 2 Passive properties of vesicles

Radius (μm)	Measured membrane capacitance (pF)	Expected membrane capacitance (pF)	Ratio of measured to expected membrane capacitance	Input resistance (MΩ)
27	85.4	91.5	0.93	0.24
20	58.5	50.2	1.16	0.46
24	60.2	72.4	0.83	0.30
27	97.1	91.6	1.06	0.45
26	78.6	85.0	0.92	0.24
27	92.7	95.0	0.98	0.08
24	60.2	72.4	0.83	0.69
27	104.9	95.0	1.10	0.46
Average values ± SEM				
25.3 ± 0.9	79.7 ± 6.5	81.6 ± 5.5	0.98 ± 0.04	0.37 ± 0.07

exponential at each of several different potentials. The time constants of inactivation so obtained are plotted in Fig. 3 *C* on a semilogarithmic scale as a function of membrane depolarization. Time constants of inactivation decreased with increasing depolarizing voltage and reached a value of 25 ms at 0 mV. The relation between time constants of decay and membrane depolarization was fitted to the sum of a single exponential and a constant τ, the limiting value of the time constant of inactivation during depolarizing voltages. The continuous line corresponds to the parameters of this function best fit to the experimental data. The upper section of Table 3 under the heading Control summarizes the activation parameters and the limiting time constant τ from several experiments. The rate of decay of K^+ currents that we observed is most likely not due to artifactual decay by the pipette glass, as described by Cota and Armstrong (1988), because we used a type of glass that causes no artifacts. In addition, we tested the effects of 10 mM EGTA

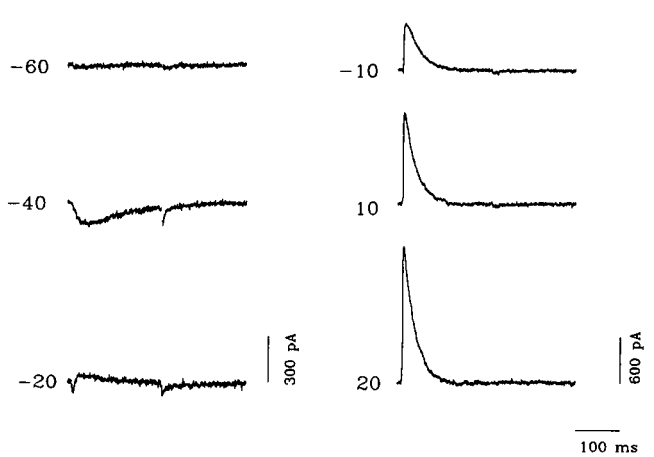

FIGURE 2 Macroscopic potassium currents in membrane vesicles. The records show currents during voltage steps to the potentials indicated (in mV) after subtraction of linear membrane components using the P/4 procedure in solutions containing K^+ (solutions B and E in Table 1). Note that the amplitude scale in right-hand records differs from that in left-hand records. E_h = −90 mV.

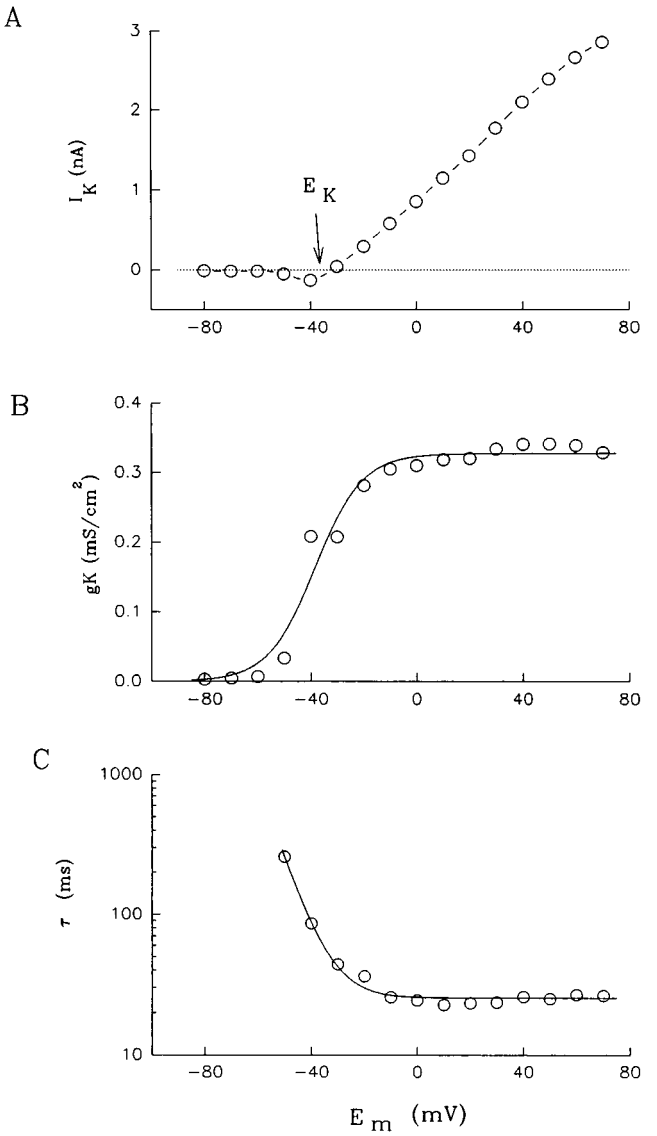

FIGURE 3 Voltage dependence of I_K currents. (*A*) The relation between membrane potential and peak current. E_K indicates the calculated K^+ equilibrium potential. (*B*) The relation between peak conductance and membrane potential. The smooth curve represents the best fit to Eq. 7, with $g_{K,max}$ = 0.3 mS/cm^2, $\bar{V}$ = −38.4 mV, and k = 8.9 mV. (*C*) The relation between the time constant of decay of I_K and membrane potential. The continuous line represents the best fit parameters of a single exponential plus a constant with a limiting value of 25.5 ms. Same experiment as in Fig. 2.

in pipette solutions on the rate of decay. Cota and Armstrong (1988) showed that the addition of this concentration of EGTA prevents the artifactual decay of K^+ currents when soft glass is used. In two experiments performed in the presence of EGTA, the mean limiting time constant was 20.7 ms, similar to the the values found in experiments with no EGTA.

Inactivation of K^+ currents was further explored in the experiment shown in Fig. 4, which shows superimposed membrane currents during pulses to +40 mV of increasing durations. Consistent with the results illustrated in Fig. 2,

TABLE 3 Activation and inactivation parameters of K^+ currents

Parameter (units)	Control value (N)	Value in presence of 4-AP (N)
Activation		
g_K (mS/cm^2)	0.29 ± 0.03 (5)	0.05 ± 0.03 (5)
$\bar{V}$ (mV)	−35.9 ± 3.6 (5)	−16.4 ± 6.5 (4)
k (mV)	6.7 ± 1.5 (5)	8.6 ± 3.8 (4)
τ (ms)	26.4 ± 2.3 (4)	—
Inactivation		
$\bar{V}$ (mV)	−66.1 ± 2.6 (4)	
k (mV)	5.9 ± 0.3 (4)	

K^+ currents inactivated during depolarizing pulses. Tail currents also decayed with increasing pulse duration, as expected from a voltage-dependent inactivation process. The decay phase of I_K during a 123-ms pulse was fitted to a single exponential, and the fitted time constant was used to construct the solid line close to the tail current records.

Unitary currents from inside-out patches revealed the presence of an ion channel with properties similar to those described above. Solutions C and F in Table 1 were used for the bath and pipette solutions, respectively. Fig. 5 *A* shows single-channel recordings currents during step depolarizations to +40 mV. Linear membrane components were subtracted from records that contained no obvious single-channel activity. As shown in Fig. 5 *A*, channel openings predominated at the beginning of the pulse and were virtually absent at later times. In Fig. 5 *B*, the ensemble average of 50 consecutive records is shown. The general characteristics of the current resemble those illustrated in Figs. 2 and 4, except that the falling phase is faster. The continuous line corresponds to the best fit of a single exponential to the decay phase of the current with a time constant of 10.5 ms, significantly lower than the value typical of whole-cell currents at this depolarization, as shown in Fig. 3 *C*. In Fig. 3 *C*, the all-points amplitude histogram is shown for the records in Fig. 3 *A*. Similar all-points histograms were constructed to measure the mean current and the single-channel chord conductance γ; in four experiments, γ = 21.3 ± 3.3 pS.

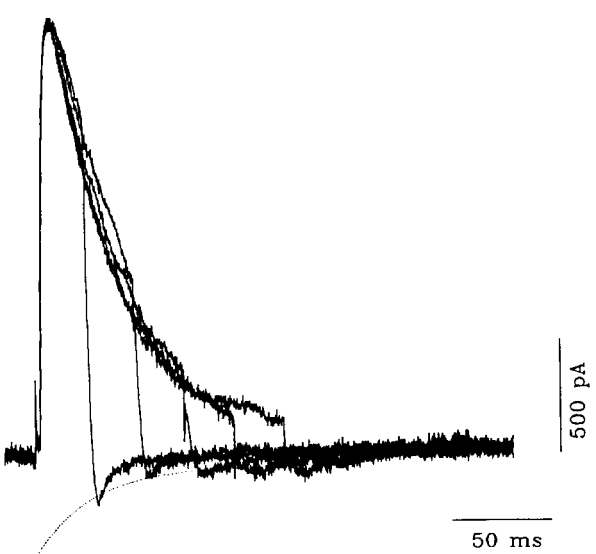

FIGURE 4 The decline of I_K during pulses to +40 mV with different durations. Records subtracted for linear components with the P/4 procedure. Note that the amplitudes of tail currents decline with a time course similar to those of I_K during the pulse. The dotted line has a time constant of 27.7 ms and was the best fit of a single exponential to the decay of I_K during a 123-ms pulse. E_h = −90 mV.

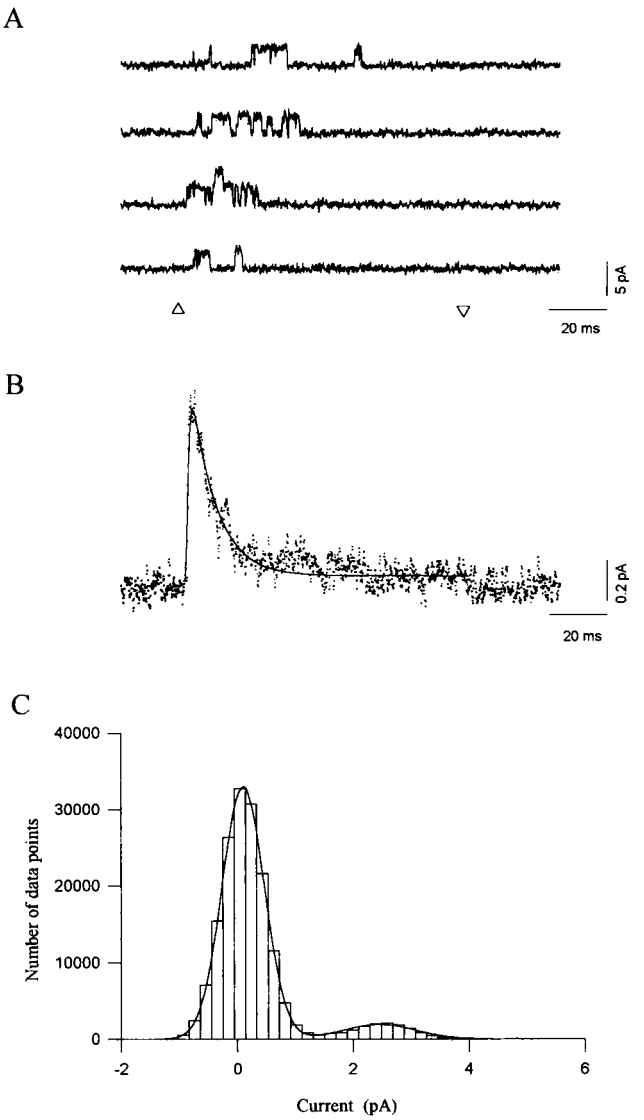

FIGURE 5 Presence of transient unitary currents in inside-out patches. (*A*) Single-channel recordings during a 140-mV pulse after subtraction of linear membrane components. E_h = −100 mV. Triangles indicate the onset and termination of pulses. (*B*) Ensemble records from the experiment shown in *A*. Responses to 50 consecutive identical pulses applied at 1-s intervals were averaged. The smooth line corresponds to the best fit of a single exponential to the decay phase of I_K and has a time constant of 10.5 ms. (*C*) All-points amplitude histogram from the experiment shown in *A*. The smooth lines represent the best fit to the data of the sum of two gaussians. The chord conductance derived from the fit is γ = 16.8 pS.

The inactivation properties of I_K were further examined in whole cell experiments with a double-pulse protocol, as first described for sodium channels (Hodgkin and Huxley, 1952). The first pulse was a prepulse of 1022 ms and variable amplitude, and the second a 100-ms test pulse to +40 mV in all cases. As the amplitude of the prepulse increased, the magnitude of I_K during the test pulse progressively decreased to zero. The relation between the value of I_K during the test pulse and the membrane potential during the prepulse was fitted to a function similar to Eq. 7, but with $I_{K,max}$ replacing $g_{K,max}$ and with $(V - E_m)$ in the exponential. This is the steady-state inactivation relation described by Hodgkin and Huxley (1952) for sodium channels that has been applied to inactivation of A currents (Rudy, 1988). Fig. 6 shows the results from an inactivation experiment with this pulse protocol. Open symbols represent the relative peak values of I_K. The continuous line is the best fit of the inactivation function with the parameters given in the legend. The inset illustrates some original records.

The lower section of Table 3 summarizes data from similar inactivation experiments. The midpoint of inactivation is close to the one found for A currents in other systems (see, for example, Segal et al., 1984).

Blockade of transient K^+ currents

A currents in other preparations are especially sensitive to blockade by 4-aminopyridine (4-AP). We observed that addition of 4-AP (5 mM) to the bath solution completely blocked the transient component of K^+ currents in vesicles. Currents in the presence of this compound only showed a remaining noninactivating outward current. This component greatly resembles the delayed rectifier K^+ current. In most experiments the amplitude of this steady component was rather small, and no K^+ currents were observed in the presence of 4-AP, suggesting that the underlying conductance is more sensitive to this compound than are the noninactivating K^+ channels. An example of exceptionally large currents in the presence of 4-AP is shown in Fig. 7 (inset). The currents activate at more positive potentials than do the transient currents, as shown in the current-voltage relation of Fig. 7.

The upper section of Table 3 under the heading "4-AP" summarizes the activation parameters of the remaining potassium currents from several experiments. These values were obtained by fitting Eq. 7 to the corresponding potassium conductance. The midpoint of activation lies at more positive potentials than that of transient currents.

Video microscopy and ultrastructure of skeletal muscle vesicles and treated muscle

Video recording of skeletal muscle fibers under collagenase treatment allowed the observation of formation of vesicles. They appeared to originate from the cell membrane, inasmuch as some of them remained attached to the surface before being released (Fig. 8 *A*). Most of the vesicles were

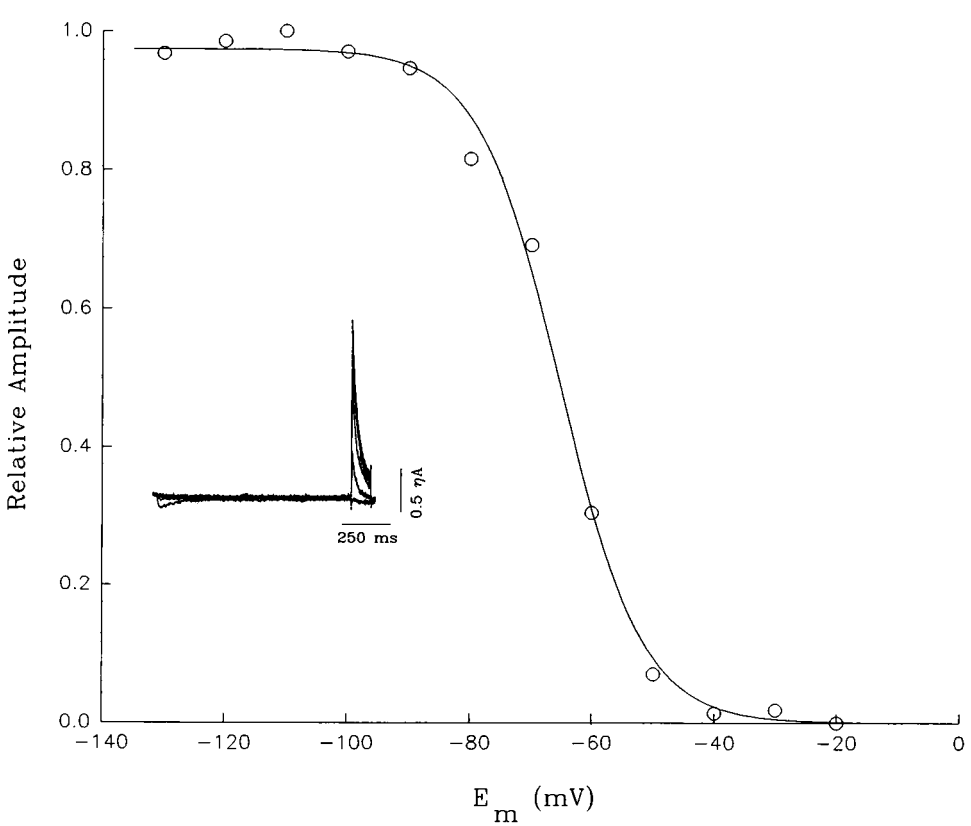

FIGURE 6 Steady-state inactivation of transient currents. The vesicle was stepped from $E_h = -100$ mV to the conditioning voltage (abscissa) for 1022 ms. Peak current in response to a test potential to +40 mV was measured and plotted relative to I_K elicited without prepulse (ordinate). The smooth line is the best fit of a Boltzmann function, with $V = -65.2$ mV and $k = 6.8$ mV. The inset shows some original records from the same experiment.

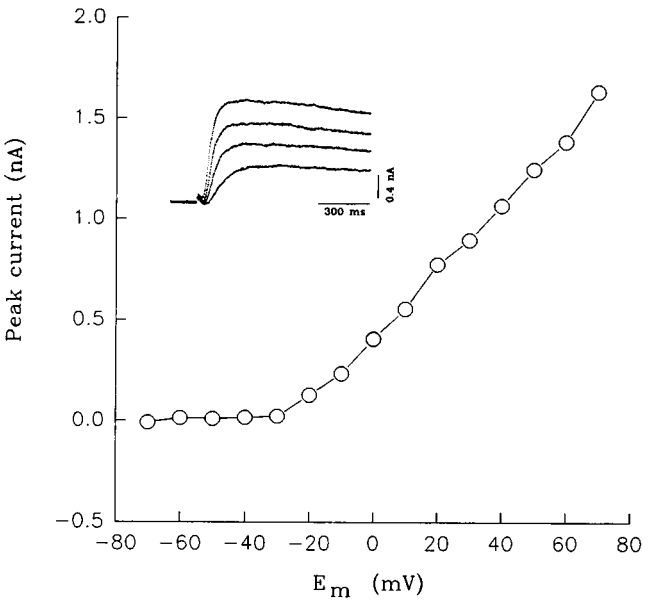

FIGURE 7 Membrane currents in the presence of 4-AP. The plot shows the relation between peak current and membrane potential. The inset shows K^+ currents in response to 100-ms pulses to several potentials from the same experiment. Linear membrane components were subtracted using the P/4 procedure. $E_h = -100$ mV.

free of internal particles, as revealed in a differential interference light contrast microscope. The size of vesicles was greatly variable and ranged from 1 to 50 μm.

Electron microscopy of vesicles showed that they were delimited by a cell membrane and confirmed that vesicles are free of cytoplasmic organelles. Some vesicles retained the external association with collagen fibers (Fig. 8 *B*). Muscle fibers treated with collagenase exhibited collagen fibrils in the process of dissociation from the cell membrane and many small vesicles on the cell surface. The sarcoplasmic reticulum was also swollen (Fig. 8 *C*).

Simulation of A currents in skeletal muscle T-system

Fig. 9 shows simulated A current records for a range of potential steps applied to the surface membrane of the simulated T-system as discussed in Materials and Methods. The time courses of the records at more depolarized potentials are not substantially different from those in the vesicles (Fig. 2). The records associated with less depolarizing voltages have different time courses than their counterparts in vesicles because much of the T-system is below E_K. The simulated currents reach a maximum of 27 nA at the highest depolarization, corresponding to a conductance of 1.5 mS/cm^2 of plasmalemma membrane. Most of the T-system was activated at these higher potentials; by increasing the lumen conductivity G_L to force the T-system to charge completely in 1–2 ms, no more than 30 nA of simulated A current could be generated.

DISCUSSION

These experiments show that it is feasible to record macroscopic currents from vesicles derived from frog skeletal muscle fibers using the whole-cell, voltage-clamp technique. The linear membrane properties measured electrophysiologically and the electron microscopy experiments revealed that the vesicles lack invaginations and have no internal organelles. These features are most convenient for voltage-clamp experiments. This preparation is therefore an alternative for the study of ion currents in skeletal muscle and is expected to provide a better voltage control than the one achieved in skeletal muscle fibers under voltage clamp. In fact, the presence of the transverse tubular system membranes greatly complicates voltage-clamp experiments in muscle. Thus, calculations have shown that the tubular membrane at the center of the fiber is far from clamped when voltage steps are imposed at the surface (Adrian and Peachey, 1973). In agreement with this conclusion, it has been shown experimentally that the potential changes across tubular membranes differ significantly in speed and amplitude from the potential at the surface (Heiny and Vergara, 1982). This lack of voltage control across tubular membranes gives rise to notches in the current records (Hille and Campbell, 1976). Another advantage is that a better control of the internal medium is probably achieved in the vesicles as compared with muscle cells. In fact, it has been shown that diffusional exchange between pipette and cell interior solutions in whole-cell experiments takes seconds to accomplish (Fenwick et al., 1982). In contrast, iontophoresis or pressure injection methods in intact muscle cells lack spatial homogeneity, and diffusion of solutions through cut ends of muscle fibers is significant only after several minutes (see for example Delay et al., 1986).

Comparison with previous work

These results show that vesicles derived from frog skeletal muscle plasma membranes develop transient potassium currents upon depolarization. The properties of these currents greatly resemble those associated with the so-called A currents recorded in many excitable cells (for reviews see Rogawski, 1985; Rudy, 1988). A currents inactivate quickly with membrane depolarization (<100 ms at room temperature), and inactivation is complete near the resting potential of neurons and other cells. We found that transient K^+ currents decay with a mean time constant of 26 ms and that the midpoint of steady-state inactivation is about -60 mV. In addition, A currents are uniquely sensitive to 4-AP (Thompson, 1977), and we found that transient currents were completely blocked by AP at millimolar concentrations.

Finally, the open probability of single-channel recordings decreases during pulses, and the single-channel conductance is similar to that of A channels (Rudy, 1988). The time course of inactivation is, however, significantly faster in the inside-out patches than in the vesicles, and the observed

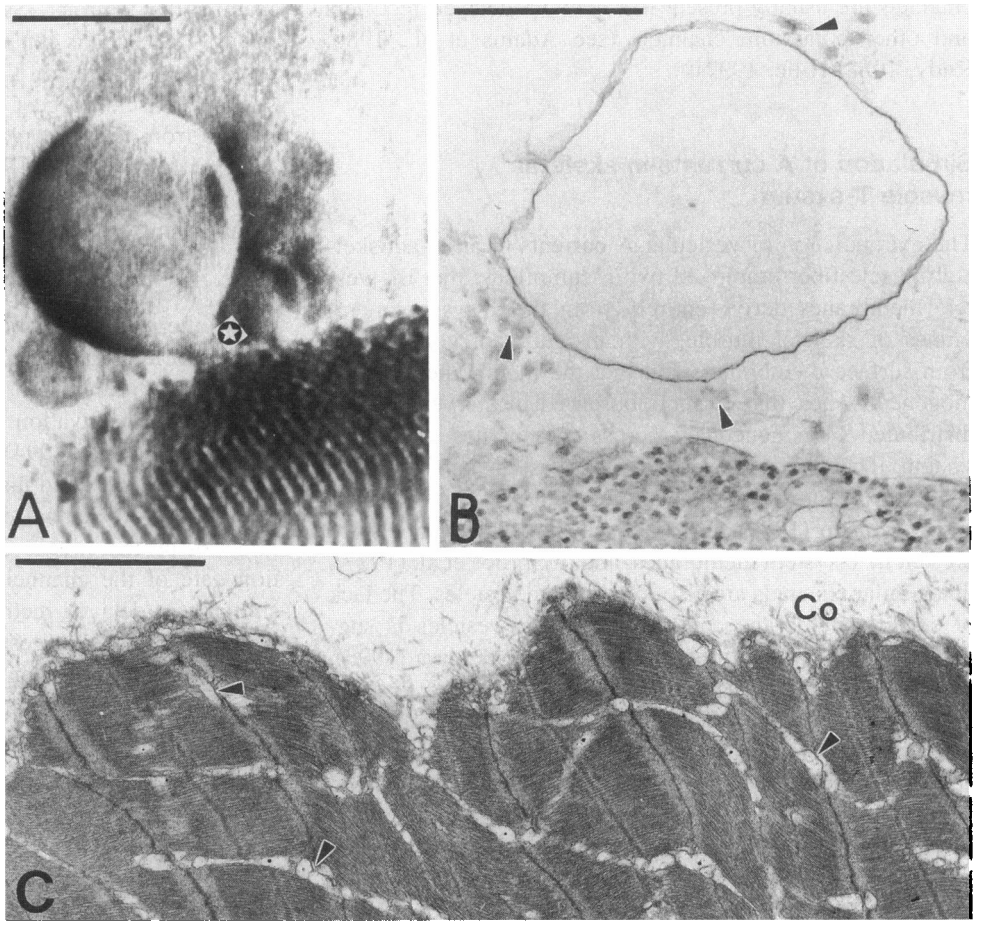

FIGURE 8 Structure of skeletal muscle vesicles. (*A*) Video images of differential interference contrast microscopy of a semitendinosus muscle in the process of releasing vesicles. Note that one vesicle is still attached to the membrane. The bar corresponds to 10 μm. (*B*) Electron micrographs that show that vesicles are formed by a typical cell membrane unit without internal cytoplasmic organelles. Collagen fibrils are associated to the external surface (arrowheads). The bar corresponds to 0.5 μm. (*C*) Collagenase-treated muscle cells presented abundance of peripheral small vesicles and swelling of sarcoplasmic reticulum (arrowheads). Co, collagen. The bar corresponds to 2 μm.

single-channel currents therefore cannot be positively linked to the macroscopic currents. However, the faster inactivation of the single channels may be related to the fact that the patches are even more isolated from environmental factors than are the vesicles, and the presence or absence of some modulatory factors in the patch preparation may have affected the time course of inactivation. As discussed below, the fact that A currents are not observed in the intact tissue strongly suggests the presence of one or more modulatory processes.

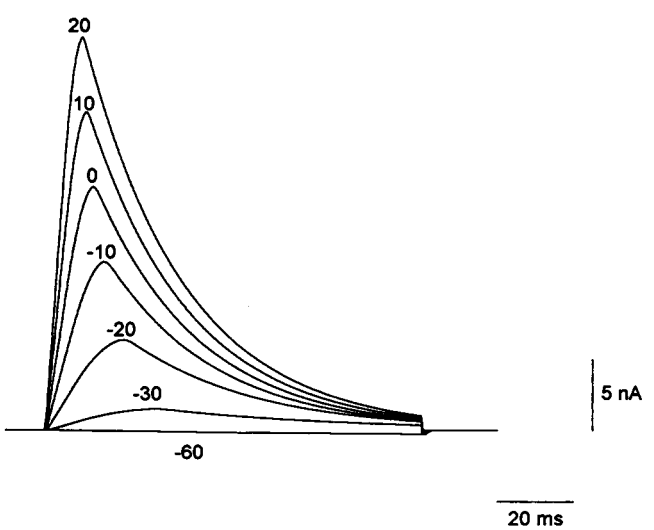

FIGURE 9 A series of time courses of simulated A currents for an intact skeletal muscle under conditions described in Materials and Methods, for 100-ms step depolarizations to the following values (in mV): −60, −30, −20, −10, 0, 10, and 20.

The inactivation properties of transient macroscopic currents described in the present experiments are clearly different from those of delayed rectifier currents of intact muscle cells. For example, Adrian et al. (1970) showed that the time constant of inactivation of delayed rectifier channels at 20°C is 0.6 s for large depolarizations. In contrast, the transient currents that we describe here decline about 25 times faster. In addition, the midpoint of inactivation is about 25 mV more negative than the corresponding value for delayed rectifier channels (Adrian et al., 1970). Although delayed rectifier potassium channels have also been studied at the single-channel level in vesicles (Standen et al., 1984, 1985), their inactivation properties have not been studied in any detail to allow a close comparison with our macroscopic data. It is clear, however, that they do not inactivate as fast as the currents that we describe, suggesting the presence of both delayed rectifier and A currents in the vesicles. In agreement, it has been previously shown that A

channels are usually present in cells with delayed rectifiers and other potassium channels (see Adams et al., 1980; Rudy, 1988; Hille, 1992).

Simulation of A currents in skeletal muscle T-system

The extrapolation of vesicular A currents to an intact skeletal muscle fiber employed two assumptions: that the vesicle membranes derive entirely from the T-system membranes of skeletal muscle, with insignificant contribution from surface membranes; and that the membranes are homogeneous, i.e., that currents observed in the vesicles are distributed homogeneously across membranes of the T-system. That the vesicles derive at least in part from the T-system is suggested by combining the results of Parent and Coronado (1989) that ATP-sensitive K^+ channels are present in T-system membranes, and of Spruce et al. (1987), that similar channels are also found in the vesicles. The lack of surface membrane contribution to the vesicles is suggested by the observations of Escobar and Vergara (1993), that vesicles do not take up fluorescent probes that are specific to the surface membrane. The numerical simulation of voltages in the T-system assumed that the A current does not significantly modify the passively propagated voltage, justified by the low current densities observed. As the main purpose of the simulation was to estimate the approximate magnitude and time course of hypothetical A currents in the T-system, the approximations to the waveforms of the A currents were deemed adequate.

When normalized to the radial surface membrane area, the simulated A currents in a skeletal muscle fiber have a conductance of about 1.5 mS/cm^2. The delayed rectifier current recorded in skeletal muscle by Stanfield (1970) had conductances of about 23 mS/cm^2. It is therefore conceivable that A currents of this small size, although present in intact fibers, remain undetected beneath the much larger I_K. However, Stanfield also made recordings in 58 mM external TEA that suppressed all but 2 mS/cm^2 of I_K, but no evidence of a rapidly inactivating current is visible in the recordings. Rogawski (1985) has shown that 25 mM tetraethylammonium does not diminish I_A, so it is not likely that the higher concentration used by Stanfield would have suppressed I_A. It is therefore unlikely that I_A is present in intact fibers.

A channels in skeletal muscle

A currents have not been observed previously in voltage-clamp experiments performed in intact skeletal muscle fibers (Adrian et al., 1970; Stanfield, 1970; Beam and Donaldson, 1983; Lynch, 1985). It is unclear why no activity of these channels is apparent in skeletal muscle as it is in vesicles. A possible explanation is that A channels are strongly inhibited by an increase in intracellular [Ca^{2+}]. This phenomenon has been observed in molluscan and mammalian neurons (Sakakibara et al., 1986; Chen and Wong, 1991) and is apparently mediated by a Ca^{2+}/calmodulin-dependent protein kinase (Sakakibara et al., 1986). In skeletal muscle, large Ca^{2+} transients produced by Ca^{2+} release from the sarcoplasmic reticulum follow membrane depolarization (Huang, 1993). If this rise in intracellular Ca^{2+} has easy access to A channels in muscle, suppression of A currents might result. Attempts to test this hypothesis by voltage-clamping vesicles using pipettes containing high [Ca^{2+}] were unsuccessful because of unstable recordings.

An alternative possibility is that the A current is suppressed or modified by ambient conditions in the myoplasm of the intact preparation. One potentially altered characteristic is fast inactivation, the hallmark of macroscopic I_A. Covarrubias et al. (1994) have reported that protein kinase C eliminates the rapid inactivation of a cloned human skeletal muscle I_A channel encoded by the gene hKv3.4. The effect of protein kinase C is to phosphorylate the inactivation gate of the channel, converting the current into one similar to a delayed rectifier, showing only slight inactivation over 1 s. The suggested scenario is that A currents may be present in skeletal muscle but are effectively masked by the removal of inactivation through ambient levels of a factor that promotes phosphorylation of the inactivation gate. Formation of the vesicles might then alter conditions and promote dephosphorylation of the inactivation gate, unmasking the I_A described here. The expression of I_A channels in skeletal muscle is plausible, because the gene hKv3.4 (previously designated Raw3) is expressed in human skeletal muscle and mediates the production of rapidly inactivating potassium currents (Rettig et al., 1992), very much like those shown in this paper.

We thank Ms. Rosalinda Flores for excellent secretarial work. JC is a graduate student of the Department of Physiology, Biophysics and Neurosciences of Cinvestav.

JC and MV were supported by fellowships from CONACyT.

REFERENCES

Adams, D. J., S. J. Smith, and S. H. Thompson. 1980. Ionic currents in molluscan somata. *Annu. Rev. Neurosci.* 3:141–167.

Adrian, R. H., W. K. Chandler, and A. L. Hodgkin. 1970. Voltage clamp experiments in striated muscle fibers. *J. Physiol. (Lond.).* 208:607–644.

Adrian, R. H., and L. D. Peachey. 1973. Reconstruction of the action potential of frog sartorius muscle. *J. Physiol. (Lond.).* 235:103–131.

Ashcroft, F. M., J. A. Heiny, and J. Vergara. 1985. Inward rectification in the transverse tubular system of frog skeletal muscle studied with potentiometric dyes. *J. Physiol. (Lond.).* 359:269–291.

Beam, K. G., and P. L. Donaldson. 1983. A quantitative study of potassium channel kinetics in rat skeletal muscle from 1 to 37°C. *J. Gen. Physiol.* 81:485–512.

Blatz, A. L., and K. L. Magleby. 1984. Ion conductance and selectivity of single calcium-activated potassium channels in cultured rat muscle. *J. Gen. Physiol.* 84:1–23.

Camacho, J., and J. A. Sánchez. 1993. Voltage-clamp experiments in skeletal muscle plasma membrane vesicles. *In* Proceedings of the Eleventh International Biophysical Congress, Budapest, Hungary. IUPAB, Budapest.

Chen, Q. X., and R. K. S. Wong. 1991. Intracellular Ca^{2+} suppressed a transient potassium current in hippocampal neurons. *J. Neurosci.* 11: 337–343.

Connor, J. A., and C. F. Stevens. 1971. Voltage-clamp studies of a transient outward membrane current in gastropod neural somata. *J. Physiol. (Lond.).* 213:21–30.

Cota, G., and C. M. Armstrong. 1988. Potassium channel "inactivation" induced by soft-glass patch pipettes. *Biophys. J.* 53:107–109.

Covarrubias, M., A. Wei, L. Salkoff, and T. B. Vyas. 1994. Elimination of the rapid potassium channel inactivation by phosphorylation of the inactivation gate. *Neuron.* 13:1403–1412.

Delay, M., B. Ribalet, and J. Vergara. 1986. Caffeine potentiation of calcium release in frog skeletal muscle fibers. *J. Physiol. (Lond.).* 375:535–559.

Escobar, A., and J. Vergara. 1993. Identificación de vesículas membranosas de músculo esquelético que proceden del sistema tubular-T. *In* Proceedings II Congreso Iberoamericano de Biofísica, Puebla, Mexico. 93. (Abstr.).

Fenwick, E. M., A. Marty, and E. Neher. 1982. A patch-clamp study of bovine chromaffin cells and of their sensitivity to acetylcholine. *J. Physiol. (Lond.).* 331:577–597.

Hagiwara, S., K. Kusano, and N. Saito. 1961. Membrane changes in *Onchidium* nerve cell in potassium-rich media. *J. Physiol. (Lond.).* 155:470–489.

Hamill, O. P., A. Marty, E. Neher, B. Sakmann, and F. J. Sigworth. 1981. Improved patch-clamp techniques for high-resolution current recording from cells and cell-free membrane patches. *Pflügers Arch.* 391:85–100.

Heiny, J., and J. Vergara. 1982. Optical signals from the surface and T-system membranes in skeletal muscle fibers. *J. Gen. Physiol.* 80: 203–230.

Hille, B. 1992. Ionic Channels of Excitable Membranes, 2nd Ed. Sinauer Associates, Sunderland, MA.

Hille, B., and D. T. Campbell. 1976. An improved Vaseline-gap voltage-clamp for skeletal muscle fibers. *J. Gen. Physiol.* 67:265–293.

Hodgkin, A. L., and P. Horowicz. 1959. The influence of potassium and chloride ions on the membrane potential of single muscle fibers. *J. Physiol. (Lond.).* 148:127–160.

Hodgkin, A. L., and A. F. Huxley. 1952. The dual effect of membrane potential on sodium conductance in the giant axon of Loligo. *J. Physiol. (Lond.).* 116:497–506.

Huang, L. H. 1993. The activation of striated muscle. *In* Intramembrane Charge Movements in Skeletal Muscle. C.L-H. Huang, editor. Clarendon Press, Oxford.

Lynch, C. 1985. Ionic conductances in frog short skeletal muscle fibers with slow delayed rectifier currents. *J. Physiol. (Lond.).* 368:359–378.

Parent, L., and R. Coronado. 1989. Reconstitution of the ATP-sensitive potassium channel of skeletal muscle. *J. Gen. Physiol.* 94:445–463.

Rettig, J., F. Wunder, M. Stocker, R. Lichtinghagen, F. Mastiaux, S. Beckh, W. Kues, P. Pedarzani, K. H. Schröter, J. P. Ruppersberg, R. Veh, and O. Pongs. 1992. Characterization of a Shaw-related potassium channel family in rat brain. *EMBO J.* 11:2473–2486.

Rogawski, M. A. 1985. The A current: how ubiquitous a feature of excitable cells is it? *Trends Neurosci.* 8:214–219.

Rudy, B. 1988. Diversity and ubiquity of K channels. *Neuroscience.* 25:729–749.

Sakakibara, M., D. L. Alkon, R. DeLorenzo, J. R. Goldenring, J. T. Neary, and E. Heldman. 1986. Modulation of calcium-mediated inactivation of ionic currents by Ca^{2+}/calmodulin-dependent protein kinase II. *Biophys. J.* 50:319–327.

Segal, M., M. A. Rogawski, and J. L. Barker. 1984. A transient potassium conductance regulates the excitability of cultured hippocampal and spinal neurons. *J. Neurosci.* 4:604–609.

Spruce, A. E., N. B. Standen, and P. R. Stanfield. 1987. Studies of the unitary properties of adenosine-5′-triphosphate-regulated potassium channels of frog skeletal muscle. *J. Physiol. (Lond.).* 382:213–236.

Standen, N. B., P. R. Stanfield, and T. A. Ward. 1985. Properties of single potassium channels from the sarcolemma of frog skeletal muscle. *J. Physiol. (Lond.).* 364:339–358.

Standen, N. B., P. R. Stanfield, T. A. Ward, and S. W. Wilson. 1984. A new preparation for recording single-channel currents from skeletal muscle. *Proc. R. Soc. Lond. B. Biol. Sci.* 221:455–464.

Stanfield, P. R. 1970. The effect of the tetraethylammonium ion on the delayed currents of frog skeletal muscle. *J. Physiol. (Lond.).* 290: 209–229.

Thompson, S. H. 1977. Three pharmacologically distinct potassium channels in molluscan neurons. *J. Physiol. (Lond.).* 265:465–488.

Vergara, J. F., and Bezanilla. 1981. Optical studies of E-C coupling with potentiometric dyes. *In* The Regulation of Muscle Contraction: Excitation-Contraction Coupling. A. Grinnell and M. Brazier, editors. Academic Press, New York.